G. Oberti, F. Bavestrello, P.P. Rossi, F. Flamigni

Rock Mechanics Investigation, Design and Construction of the Ridracoli dam

(reprinted from *Rock Mechanics and Rock Engineering XIX,* 3, july - september 1986)

ismes s.p.a.
viale Giulio Cesare, 29 - 24100 BERGAMO - tel. 035/358111 - telex 301249 - BG

Rock Mechanics
and Rock Engineering 19, 113—142 (1986)

Rock Mechanics
and Rock Engineering

Rock Mechanics Investigations, Design and Construction of the Ridracoli Dam

By

G. Oberti, F. Bavestrello, P. P. Rossi
ISMES Bergamo, Italy

F. Flamigni
Consorzio Acque, Forlì, Italy

Summary

The Ridracoli arch-gravity concrete dam is the major work in a multipurpose project whose main scope is the water supply to 37 communities in the Forlì and Ravenna Provinces.

The particular geological and structural characteirstics of the foundation rock mass, consisting of a rhythmical alternation of sandstone, silstone and marl, required a wide program of in situ and laboratory investigations in order to obtain a detailed physical and mechanical characterization of the foundation.

The design criteria based on the use of a physical and mathematical model are illustrated as well as the limit equilibrium analysis of the stability conditions of the abutments. Particular attention has been devoted to the problem of the excavation stability; excavation methods and stabilizing works are illustrated in detail. The seepage problems are also presented with the description of grouting and drainage works.

1. Introduction

The Ridracoli arch-gravity concrete dam closes off a very wide U-shaped valley at the confluence of the river Bidente with the Celluzze mountain stream about 50 km from the town of Forlì, in the Tuscan-Romagna Appenines in Italy.

The dam (Fig. 1) consists of a double-curvature arch structure, almost symmetrical in relation to the main section plane, resting on a pulvinus along the total length of the excavation profile.

Main characteristic data:

— Storage capacity	30×10^6 m^3
— Power generation	35 Gwh
— Crest Elevation	561.00 m a. s. l.
— Maximum water level	557.30 m a. s. l.
— Maximum height	103.50 m

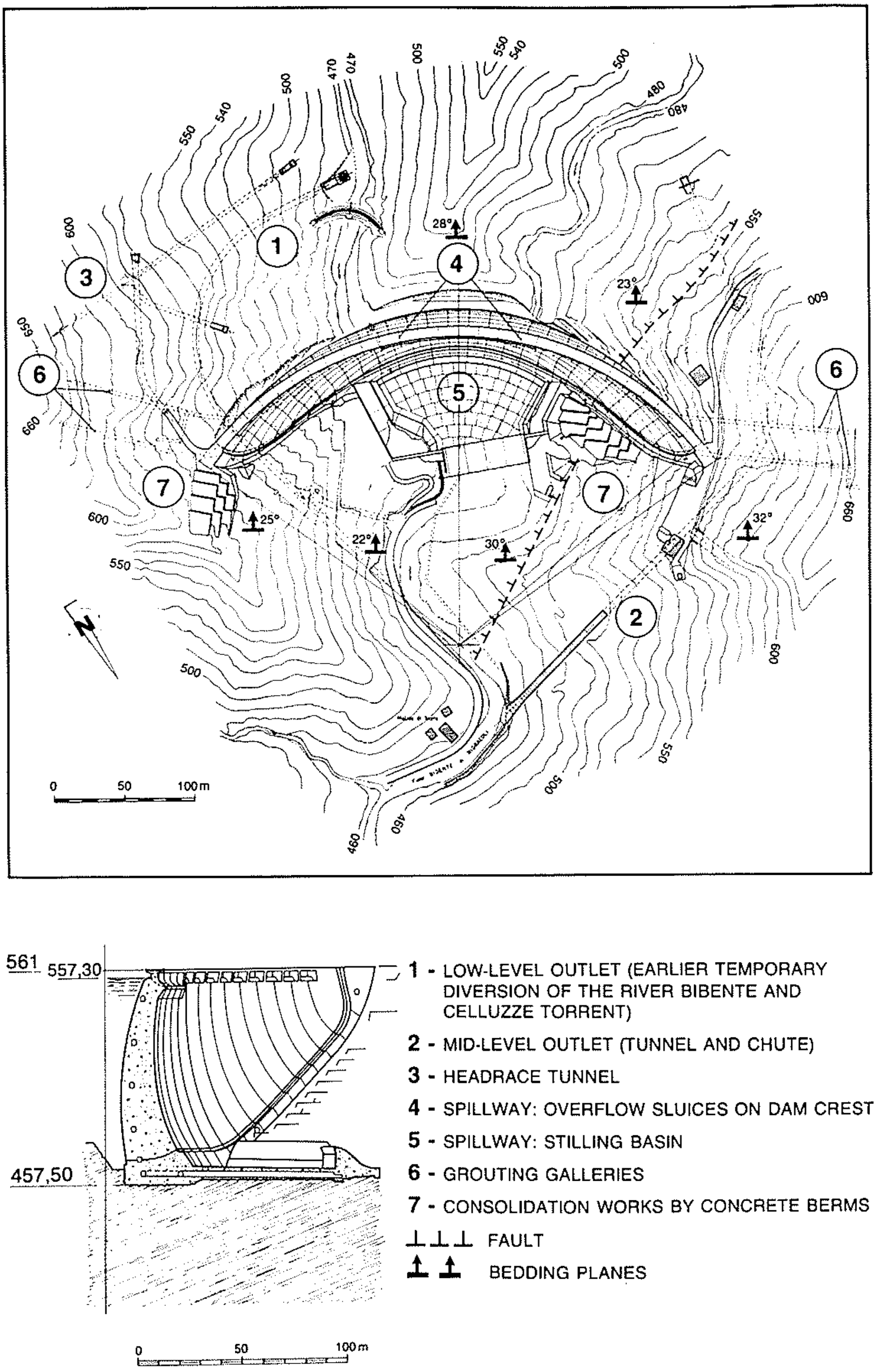

Fig. 1. Layout and main section of the dam

— Longitudinal development of the crest	432.00 m
— Ratio between chord of crest arc and max height of the dam	3.3
— Volume of the dam	590 000 m^3

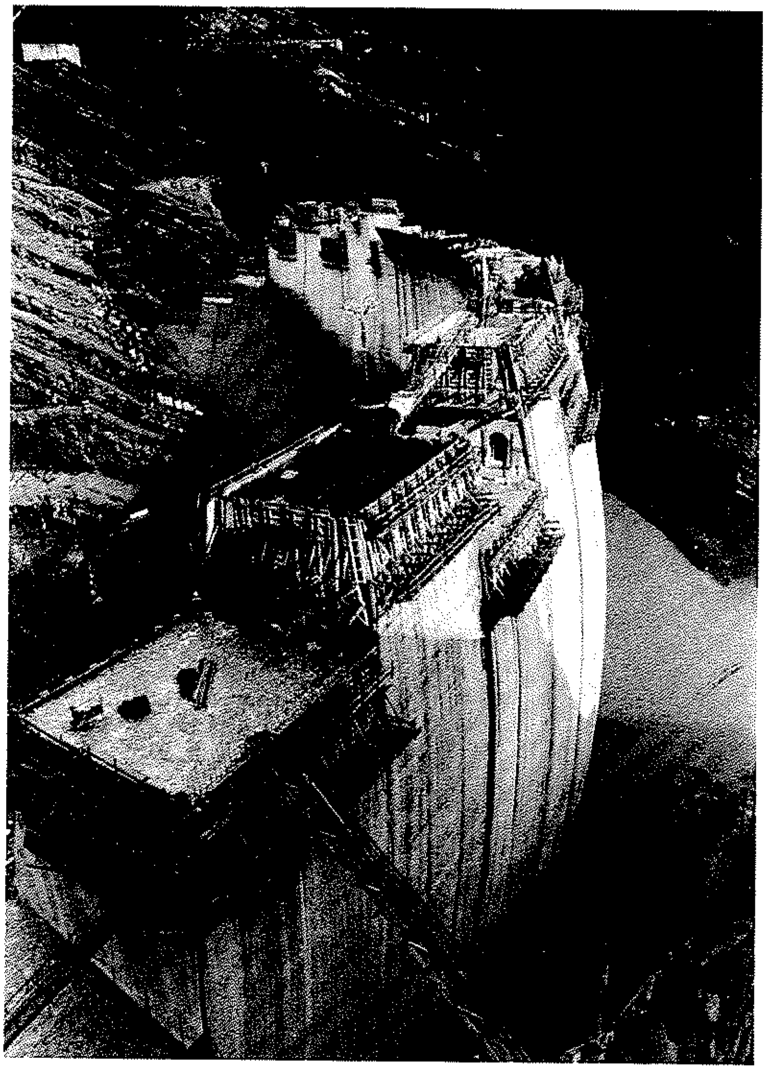

Fig. 2. View of the dam during construction

The storage reservoir is intended for water supply to 37 communities in the Forlì and Ravenna Provinces, including the main towns and the San Marino Republic.

Construction work, entrusted to Coridra General Contractor (Joint Venture including Cogefar, Milan; C. M. C., Ravenna; and Lodigiani, Milan) was started in the spring of 1975 and completed in the spring of 1982. Fig. 2 shows a view of the dam during construction.

The design was performed by Alpina S. p. A., Milan, under the guidance of the first author as responsible for the design of the dam.

Construction supervision was entrusted to ELC-Electroconsult, Milan.

2. Geology

A marl-sandstone formation of Miocene outcrops all over the reservoir area and at the dam site. This formation is over 5 000 m thick and consists of a rhythmical alternation of sandstone (44%), siltstone and marl (56%). Each marl-sandstone sequence has a thickness variable from a few decimeters to over 7 m, and exhibits a great continuity with respect to the

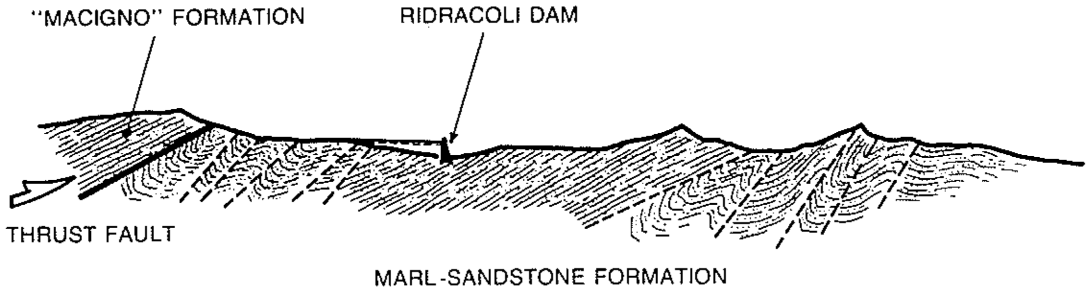

Fig. 3. Geological section

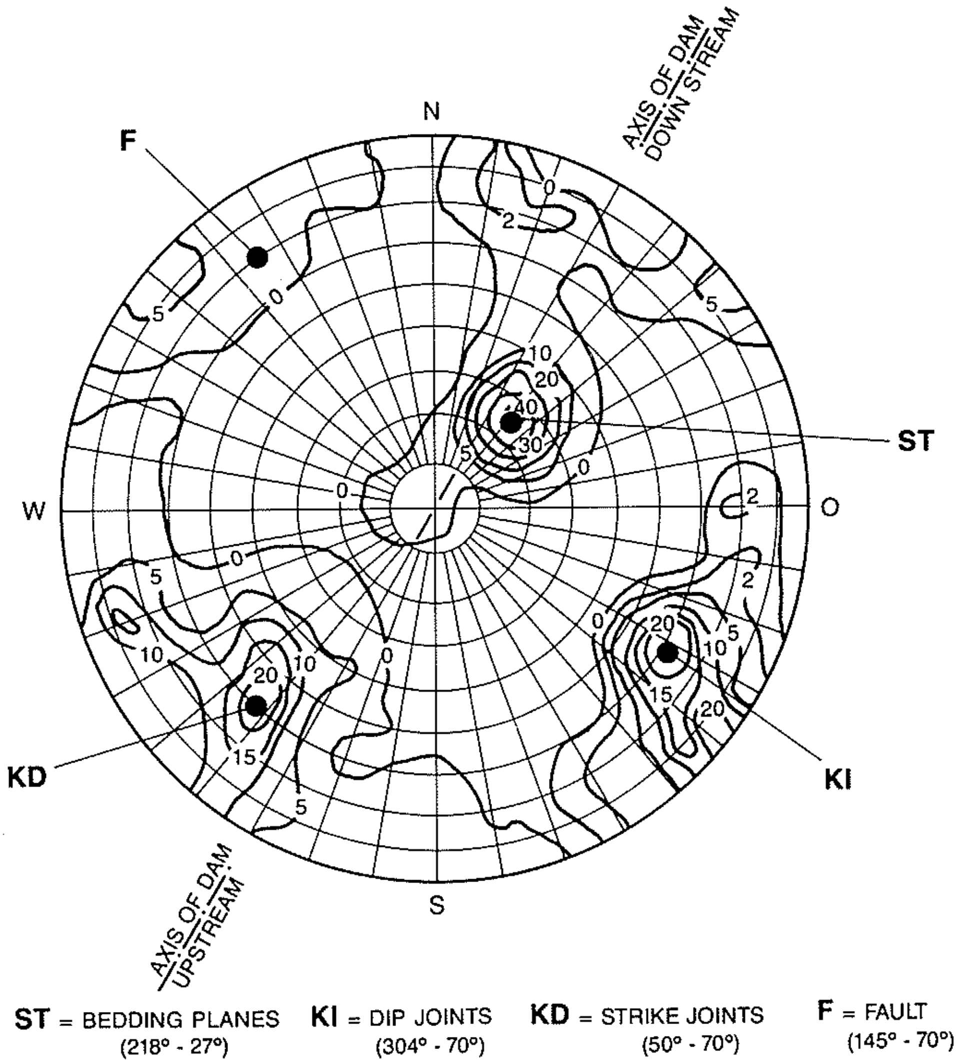

Fig. 4. Polar diagram of the main structural systems using lower hemisphere

bedding planes. Some intercalation layers of laminated and foliated marl are present, as well as thin layers of secondary calcite which is highly striated according to the dipping towards south-west with a regular monoclinal pattern.

Fig. 3 shows a geological section along the river Bidente valley. It may be noted that at the dam site this formation presents a quite regular stratification. Two faults (6 km apart) are clearly visible upstream and downstream of the dam. They have greatly disturbed the formation and given rise to numerous minor faults. One cross fault including a 1.5 m wide zone of fractured rock and an earth filling constitutes the only structural element at the dam site along which appreciable displacement has occurred (throw about 40 m).

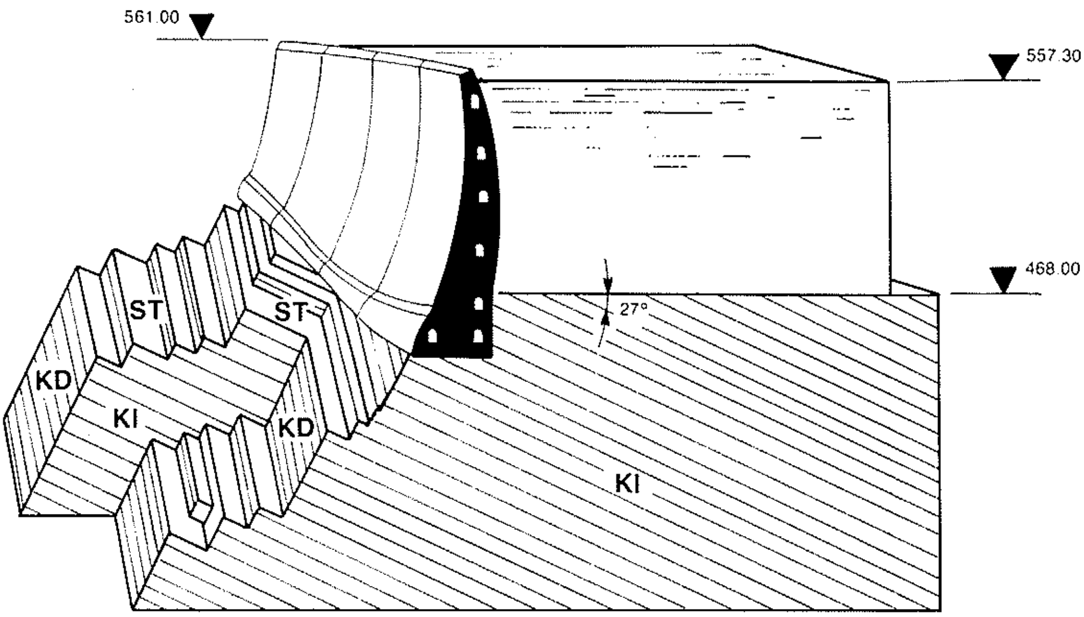

Fig. 5. Isometric view of main joint systems

The structural scheme of the dam foundation rock mass was determined by a detailed stratigraphic survey of 600 layers and by many core drillings about 80 m deep. Core recovery was 90—100% and *RQD* index was 70—90%. The main joints of the rock mass illustrated in the polar diagram of Fig. 4 are the following:

— a system of stratification joints (*ST*) striking upstreamwards relative of the dam axis by 218°, with a dip of 27°;
— two systems of subvertical joints chiefly involving sandstone, one of which (*KI*) having nearly the same direction as the valley axis, and the other one (*KD*) being almost perpendicular to the previous one.

These subvertical joints have openings of 1 to 3 mm, filled with calcite and at times with clay only in the most decompressed and surface areas. The main joint systems of the rock mass with respect to the dam are shown in the simplified structural scheme of Fig. 5.

Joint systems were studied with special attention by a detailed photogrammetic survey at the dam site, after the rock substratum was uncovered. Three typical layers, characterized by the presence of foliated and laminated marl, with thickness of a few centimeters, were found. The shear strength parameters along these joints have very low values.

3. Physical and Mechanical Characterization of the Foundation Rock Mass

3.1 In Situ Investigations

Given the importance of the dam and the particular geomorphological features of the foundation rock, it was deemed advisible to carry out a special investigation campaign (Rebaudi, 1978) in order to make it possible also to statistically ascertain and appraise the basic design parameters. The aim of this investigation campaign was to obtain clear and detailed information concerning the following aspects:

— structural characteristics of the rock mass,
— deformability and strength parameters,
— hydrogeological problems.

Several investigation phases were carried out including:

— 20 rotary core drillings (depth 60 to 80 m) with a total length of 1 300 m;
— 4 exploratory adits of a total length of 220 m; one at the right abutment, two on the left (to locate the fault) and one in the river bed area;
— 1 exploratory shaft in the river bed area (to locate lower laminated layers);
— geophysical surveys;
— 14 plate bearing tests in the adits in directions parallel and normal to the stratification;
— 2 deformability tests by means of a hydraulic pressure chamber;
— 6 flat-jack tests in the adits (right and left abutment);
— 13 shear tests on stratification joints;
— permeability tests (about 200);
— groutability tests.

3.1.1 Geophysical Surveys

To evaluate the uniformity of the rock, a geophysical survey covering the entire perimeter of the foundation was carried out by means of sonic log and cross-hole methods up to a depth of about 80 m using the existing boreholes.

The sonic velocity measured by means of the cross-hole method showed rather high values (between 4 000 to 5 000 m/s) which were quite uniform along all the perimeter of the foundation.

Really interesting results were also obtained by sonic log measurement which agreed well with the stratigraphic survey showing clear and regular variation of velocity according to the layer sequence.

3.1.2 *Deformability Tests*

Plate Bearing Tests

Several plate bearing tests were carried out in some sections of the exploratory adits. These tests were performed both perpendicular and parallel to the stratification, using 60 cm-diam circular flat jacks having a uniformly distributed pressure up to a max value of 6 MPa. The use of flat

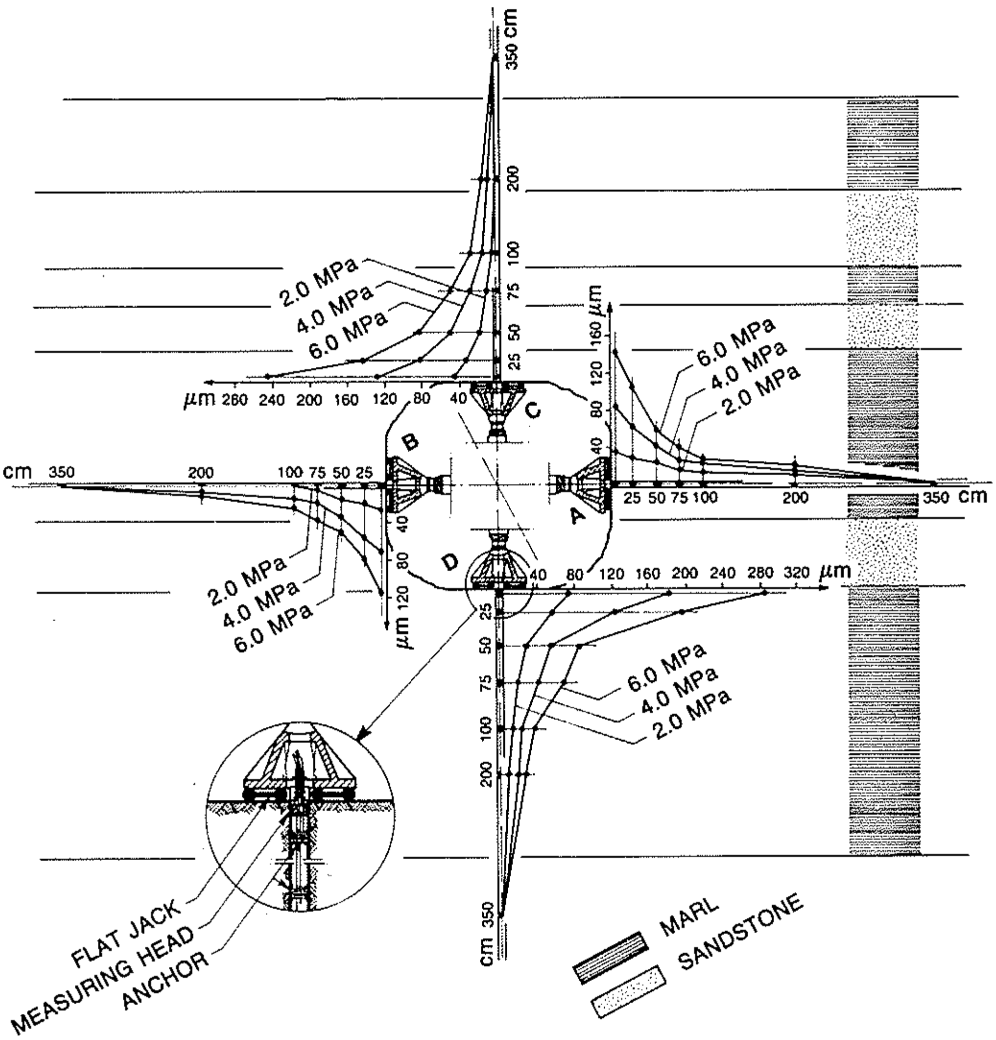

Fig. 6. Plate bearing tests parallel and perpendicular to the stratification. Diagrams of deformations as a function of the depth

jacks directly applied to the rock surface, which has first to be given a level smooth surface, makes it possible to obtain a uniform pressure distribution which reproduces, with a very good approximation, the theoretical behaviour of a perfectly flexible plate. Deformations were measured by means of special multiple-point extensometers, installed inside 75 mm-diam boreholes drilled in the centre of the loading surfaces.

Fig. 6 shows deformation diagrams obtained for a typical section of the exploratory adit in which two loading tests were performed (one perpendicularly and the other parallel to the stratification). These deformations were plotted in the diagram as a function of their depth for three different values of the applied pressure (2, 4, 6 MPa).

The measuring technique used makes it possible to assess the deformability modulus of the undisturbed rock mass above the loosened rock layer around the exploratory adit. The thickness of this loosened layer was about 500 mm as could be shown by sonic velocity and sonic logging tests carried out inside boreholes drilled in the centre of the loading surfaces.

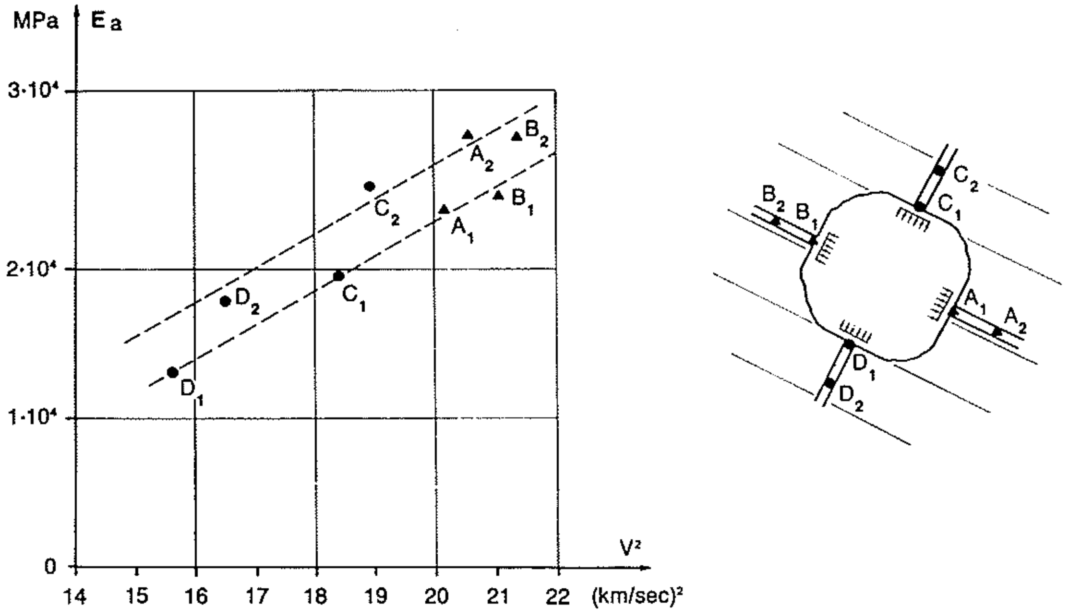

Fig. 7. Plate bearing tests on a section of right bank exploratory adit. Correlation between deformability modulus (*E*) and square of sonic velocity (V^2) measured at different depths from the loading surface (0.07 and 0.50 m)

Measurements of the sonic velocity (*V*) performed inside the boreholes have been compared with deformability moduli *E* obtained by means of plate bearing tests. In each borehole two velocity measurements were performed with the source equipment installed at a depth of 3.50 m and two receivers installed at different depths (0.07 and 0.5 m). Fig. 7 shows the correlation between *E* and *V* obtained in a test section from the right bank (Oberti et al., 1979).

Tests by Hydraulic Pressure Chamber

The presence of rock layers of great thickness (up to 2 m) led to the use of a testing technique able to determine the deformation behaviour of a rock mass on volumes of considerable size. To this end, the hydraulic pressure chamber testing technique was used applying to the wall of the 3 m-diam exploratory adit a uniform hydrostatic pressure up to 4 MPa over an 8 m length. Two tests were carried out on the right and left abutments according to the scheme of Fig. 8.

The testing technique (Rossi, 1980) has recently been improved as regards the loading and measuring systems; deformations were measured at the central section of the chamber by means of multiple-point extensometers installed inside radial boreholes drilled perpendicular and parallel to the stratification surfaces. Deformations recorded during the test on the left bank are given in the diagrams of Fig. 9, as a function of depth, for several values of the pressure applied to the adit surface.

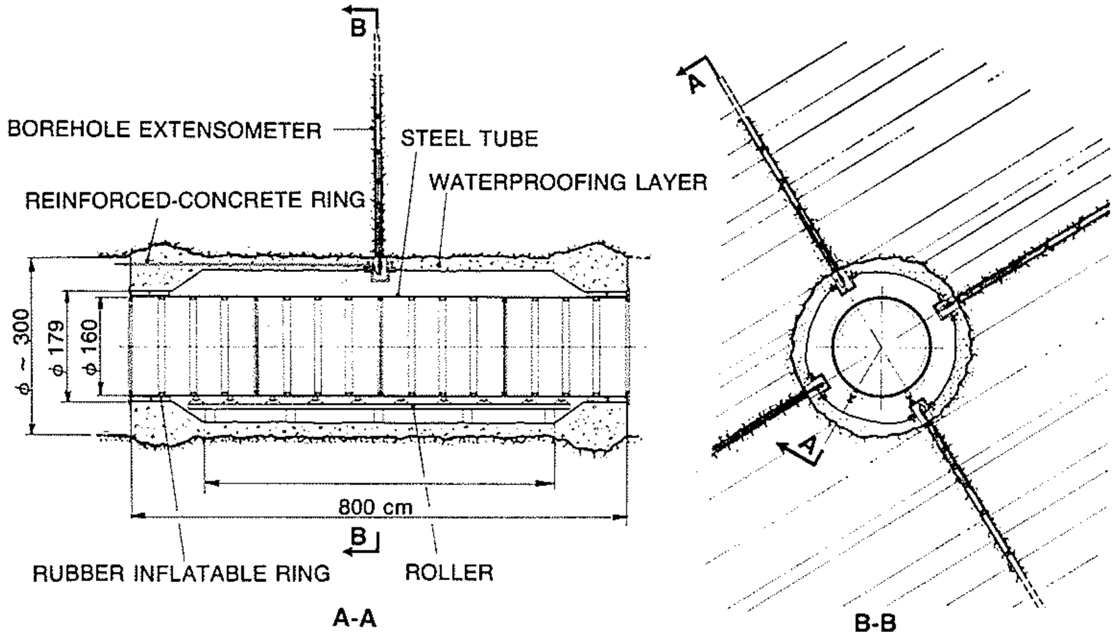

Fig. 8. Scheme of the hydraulic pressure chamber test

A typical stress-deformation diagram obtained on the left abutment is shown in Fig. 10. The deformations, measured in a direction perpendicular to the stratification at a depth of 0.50 m from the surface of the adit, are relative to the undisturbed rock mass above the loosened layer.

The average values of reversible moduli (Er) determined in the directions parallel and perpendicular to the stratification and relative to the max stress level applied by the dam (dashed line of Fig. 10) are shown in Table 1. In the same table the corresponding values of reversible moduli obtained by means of plate bearing tests are presented.

Table 1. *Comparison Between Average Reversible Moduli Relative to a Stress Level of 3 MPa*

	$Er\,//$ (MPa)	$Er \perp$ (MPa)
Hydraulic pressure chamber	18 000	16 000
Plate bearing test	24 000	18 000

Table 1 clearly shows that the ratio between $E//$ and $E\perp$ determined by pressure chamber test is lower than that determined by plate bearing test.

The diagrams of Fig. 11 show the values of ratio $f1/f2$ between the deformations measured by pressure chamber test perpendicular and parallel to the stratification versus depth. It may be pointed out that above a 0.50 m-deep surface layer, where a marked loosening of the rock strata is noted, the ratio $f1/f2$ exhibits quite low values (between 1.1 and 1.2). These values are lower than those obtained by plate bearing tests, where the ratio between the deformation perpendicular and parallel to stratifications is on average between 1.3 and 1.4 (Oberti et al., 1983).

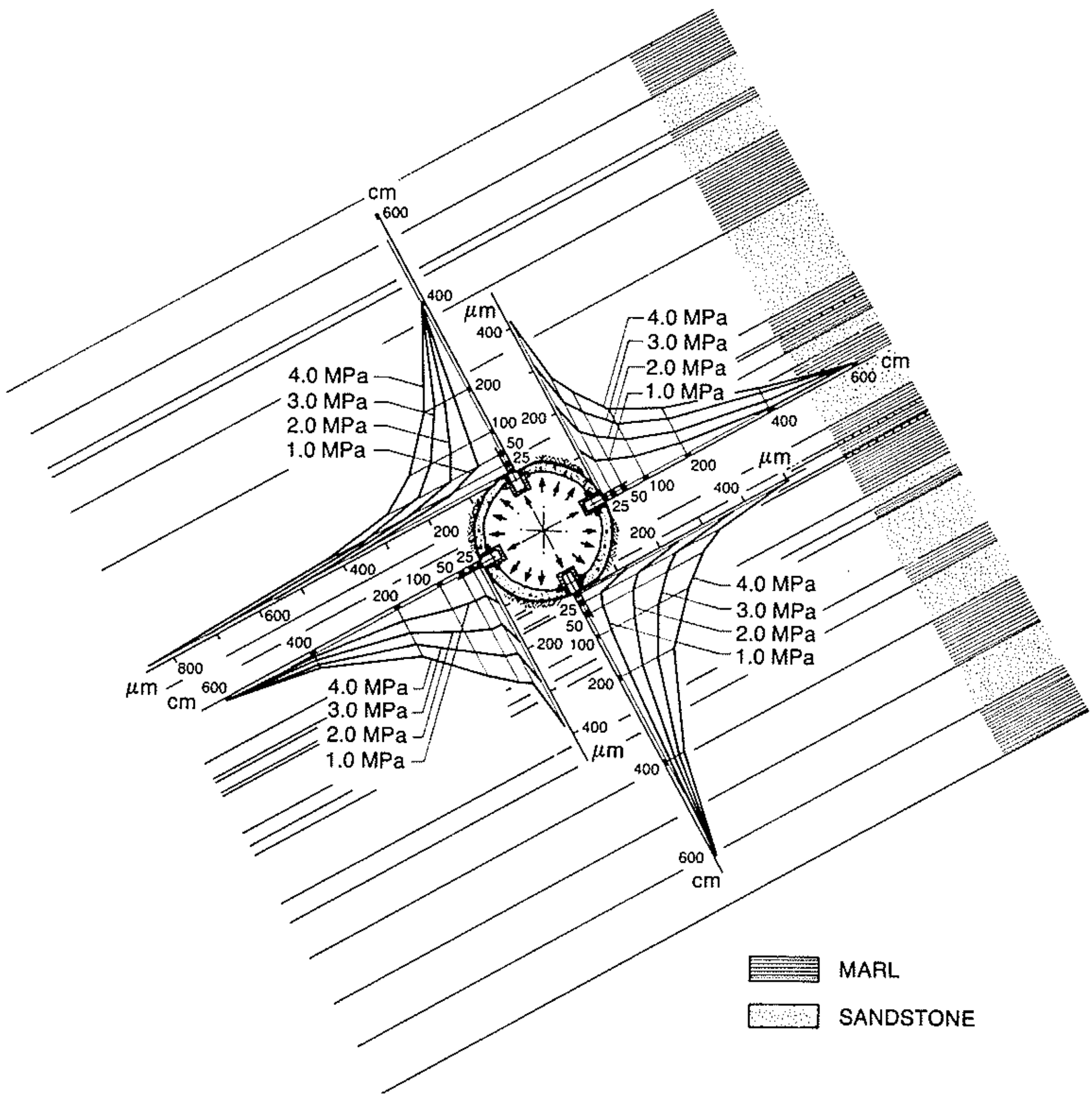

Fig. 9. Hydraulic pressure chamber test on the left abutment. Diagrams of the deformation as a function of the depth

It was observed that the values of deformability modulus which take into account the total deformability of the rock mass in the loading phase are about 30% lower than the reversible ones.

For the design of the dam it seemed advisible to assume, as design parameter, the value of the total deformability modulus of the rock mass in order to take into account the effect of several loading cycles. For this

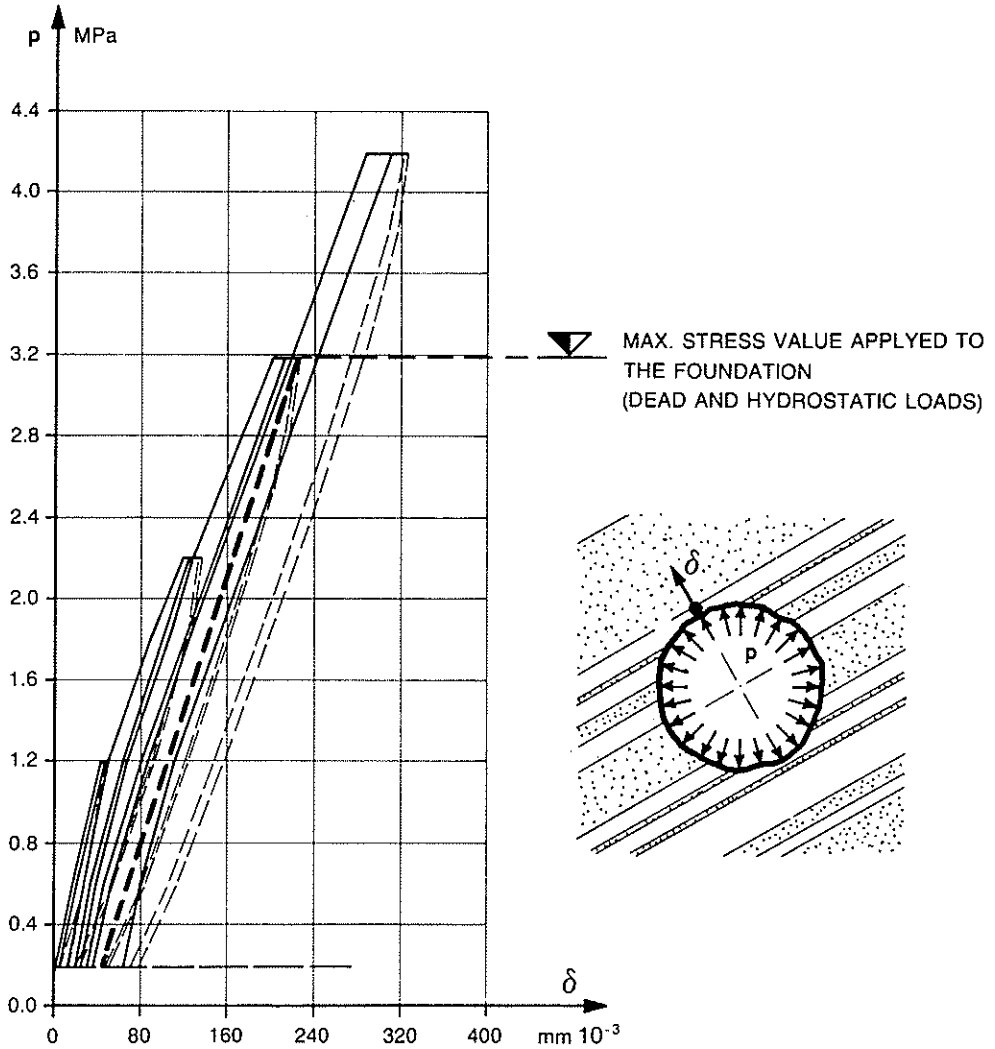

Fig. 10. Typical stress deformation diagrams obtained by hydraulic pressure chamber test.

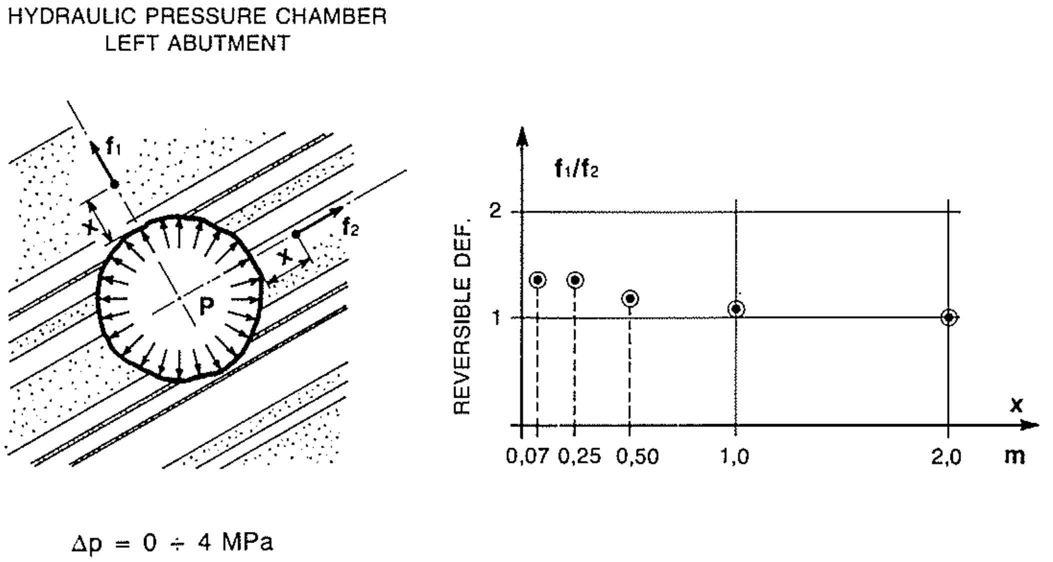

Fig. 11. Values of the ratio $f1/f2$ between the deformations measured in direction perpendicular and parallel to the stratification

reason a value about 10000 MPa was assumed for deformability modulus in both directions (normal and parallel to the stratification) mainly on the basis of the results of hydraulic pressure chamber tests.

Flat Jack Tests

Numerous flat jack tests were carried out on the thicker marl layers (> 1 m) both on the right and left bank. These tests aimed firstly to determine in situ deformability properties of marl in direction perpendicular to the bedding planes, and the state of stress existing at test points. Subsequently, flat jack tests were performed to determine rheological properties of the marl lithotype, by means of long term (some 50 days) loading tests. A 10 MPa pressure (about 3 times the maximum stress induced by the dam) was applied to each flat jack (1 m × 0.50 m) and the pressure was kept constant during the whole duration of testing using hydropneumatic accumulators. Deformations were measured by means of displacement transducers connected to automatic recorders.

Under these very conservative testing conditions a creep deformation of about 60—70% of the instantaneous one was measured.

3.1.3 Shear Tests

Special attention was given to determining the strength along stratification joints, which, as will be explained further on, represented a critical parameter for the stability analysis of dam abutments.

Six shear tests were carried out into the exploratory adits, on the left and right banks. A remarkable variation was observed depending on the type of stratification joint, from a minimum friction angle $\varnothing = 13^0$ for contact between sandstone and laminated-clayey marlstone to an angle $\varnothing = 26^0$—35^0 for contact between sandstone and marl. An additional 7 shear tests were carried out at the surface of the right abutment, to throughly investigate the mechanical characteristics of the contact between sandstone and laminated-clayey marlstone.

These tests were carried out on blocks (0.50 × 0.50 × 0.35 cm) cut in a layer of sandstone which forms the roof of the laminated stratum.

The results of these tests (see Fig. 12), carried out with two constant values of normal load, verified the low value of friction angle $\varnothing = 13^0$ and showed that the cohesion is of the order or 0.2 MPa. The residual strength is slightly smaller than the peak one and sometimes practically coincident. Therefore, the behaviour of the joint may be assumed to be elasto-plastic.

The displacements needed to reach the maximum shear strength are very small, about 1—2 mm.

3.1.4 Permeability and Groutability

The marl-sandstone formation may be considered, as a whole, to be slightly permeable, as the paths of seepage are limited to discontinuities involving almost exclusively the sandstone strata. Thus a marked anisotropy of the permeability was expected with a maximum along the stratum and a minimum normal to it.

Lugeon tests were carried out in 5 m sections of the boreholes in a direction normal to bedding planes. The permeability coefficients were evaluated as follows:

$K=4\times10^{-7}$ m/s down to a depth of 30 m; (3.8 Lugeon)
$K=2\times10^{-7}$ m/s down to a depth of 55 m; (2.4 Lugeon)
$K=10^{-7}$ m/s for greater depths. (1.5 Lugeon)

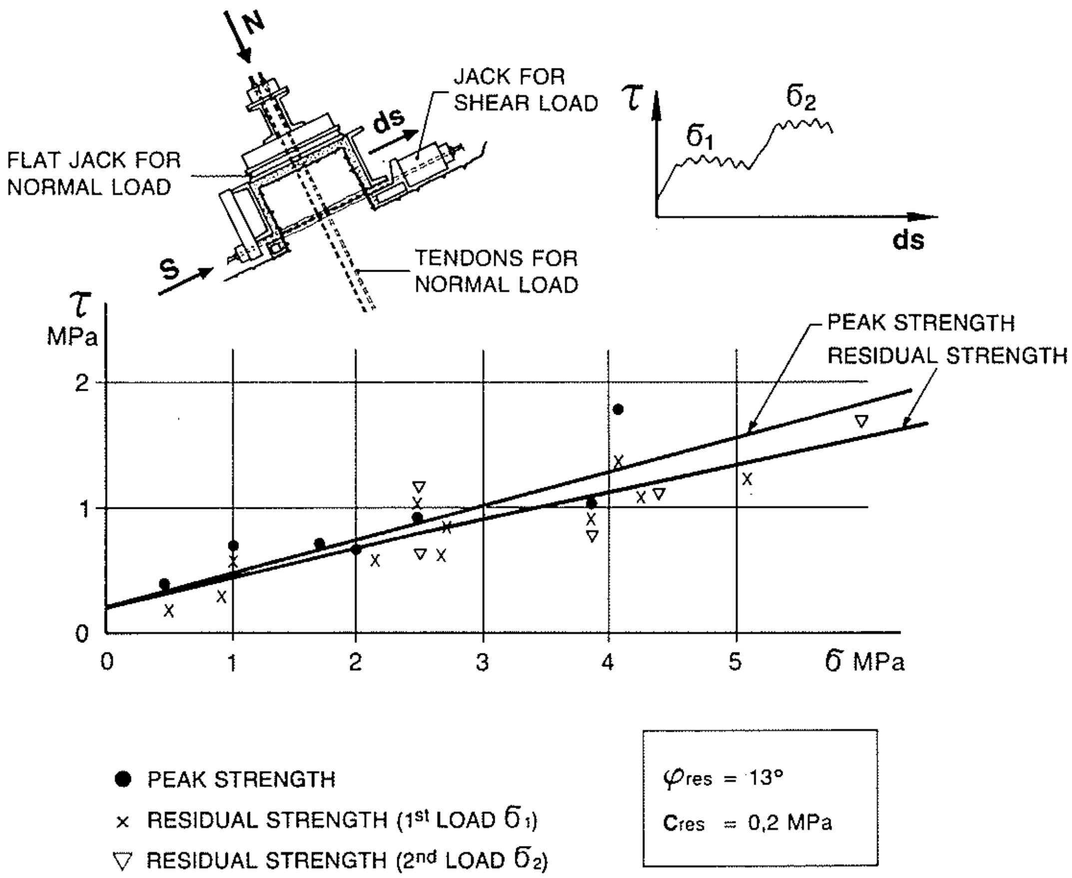

Fig. 12. Shear test carried out on laminated layers

Directional permeability tests, carried out from the bottom of the adit excavated at the right abutment to define the permeability along sandstone strata, showed an average value higher than the previous ones and equal to $K=5\times10^{-6}$ m/s.

To determine the groutability characteristics, a lot of tests were carried out down to a depth of about 70 m (Rebaudi, 1978). The average absorption was very low (550 N/m), even if the pressures applied for experimental purposes, were relatively high (from 0.5 to 3.0 MPa increasing with depth). Permeability check tests showed a decrease of coefficient K, sometimes over 80%.

The relevant improvement of the elastic characteristics was checked by geophysical measurements (cross-hole and sonic log). A general increase of sonic velocity minimum peaks on the order of about 200 m/s was observed.

On the basis of the results of the aforementioned tests the characteristics of the grout curtain were defined in order to reach a depth where the natural permeability of the rock mass was not higher than 1 Lugeon Unit This depth was found to be approx. 75 m.

3.2 Laboratory Tests

3.2.1 Mineralogical and Petrographical Tests

Mineralogical and petrographical tests were carried out on typical selected samples of a sedimentary sequence, which is repeated in the formation with very similar characteristics.

These tests showed that:

— the sandstone has an essentially calcitic cement which confirms the character of the hard rock identified by the macroscopic examination;

— the marl has a quartzose-feldspar mineral content, embedded in the "marly" matrix, composed of calcite and clay minerals, which have a great influence on the mechanical characteristics. In this sense, the percentages of calcite in the matrix are significant, being much higher than those in the total of the marl ($CaCO_3$: 60% in the matrix, 46% in the total).

3.2.2 Uniaxial and Triaxial Compressive Tests

A wide investigation was carried out to determine the mechanical characteristics of the different lithotypes particularly on the marl and siltstone. Over 200 undisturbed samples were cored from the foundation area by means of a triple sampler equipped with a PVC pipe, so that the samples were kept in their natural humidity conditions. Uniaxial and triaxial compressive tests were performed on marl and siltstone lithotypes to study the deformability and strength characteristics as a function of the orientation of specimen axis in relation to the bedding plane. Samples were taken with three different inclinations (α) in relation to the bedding planes, such as $\alpha = 0^0$, 30^0, 45^0.

The results of tests carried out with the following confining pressure values of 0—2.5—5.0—10—15 MPa are summarized in the diagram of Fig. 13, which shows the average values of compressive strength versus confining pressure ($\sigma_2 = \sigma_3$) for different values of angle α. A marked decrease of strength is noted when α increases from zero to 45^0. Such a decrease is more evident for low values of the confining pressure.

Additional uniaxial compression tests have been carried out in order to determine the strength characteristics of marl after 20 loading cycles (between 0 and 6 MPa) and after 10 wetting and drying cycles. It was observed that these severe testing conditions determine only a slight decrease of uniaxial strength (less than 20%).

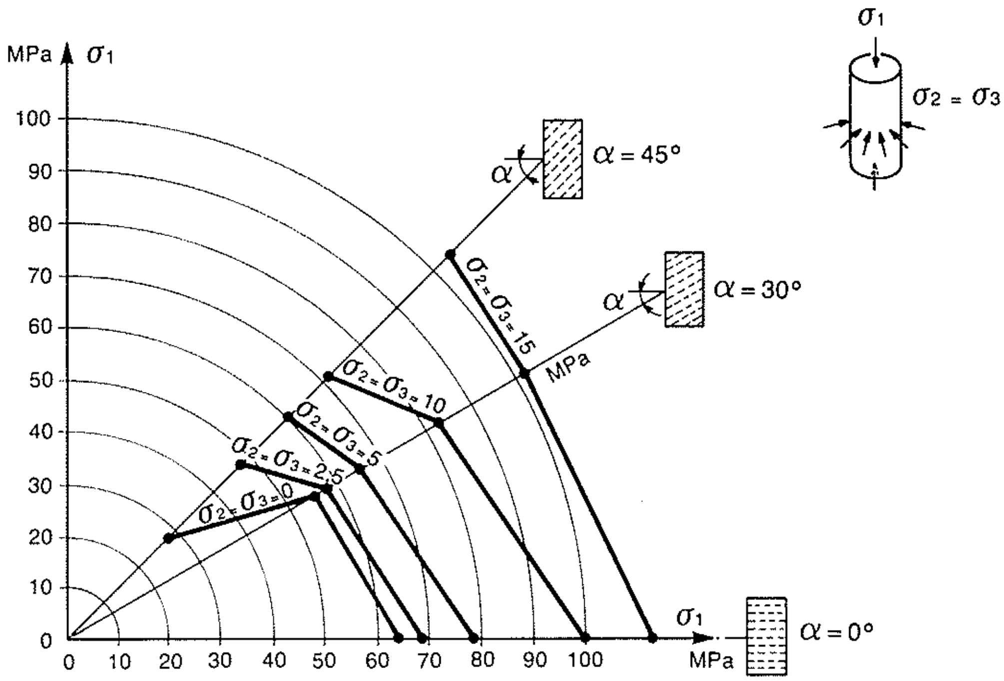

Fig. 13. Triaxial tests on marl specimens

4. Analysis of Dam Foundation Mechanical Behaviour

On the basis of the results obtained by the previously described studies, the values of the parameters necessary for the design of the foundations were determined. At first, a preliminary design of the dam was made by means of the Tolke method; the elastic deformability of the foundation rock mass was introduced (Vogt, 1925).

Then an elastic 3D-FEM model (13 000 degrees of freedom) was performed in order to investigate the behaviour of the dam and of a large foundation volume. In this model the fault plane crossing the abutment at el. 490 m was also simulated (Fig. 14).

4.1 Physical-geomechanical Model

A verification of the definitive design solution was carried out by means of a physical model (see Fig. 15) in order to evaluate the interaction between the structure and its complex foundation up to failure and to check the global stability conditions of the foundation rock mass (Fumagalli, 1977). This model was built in a geometric scale 1 : 100 by using materials with deformability and strength characteristics reduced to 1 : 2.4 scale ratio. The bedding planes were reproduced including the three typical laminated layers. The following values of friction angle on the bedding planes were reproduced: $\varnothing = 13^0$ at the laminated layers, and $\varnothing = 24^0$ at the other joints. Zero cohesion was reproduced at all joints. A dead-weight system (applied with steel rods) was extended to the whole rock foundation.

During the test at normal loading conditions, settlements along laminated layers were observed, especially along the lower laminated layer under the bottom of the dam. Part of these settlements was absorbed by the dam foundation as permanent deformations. This effect was also emphasized by the displacement of the main cantilever and was fairly evident also at lower levels, with an inclination that is very close to bedding planes.

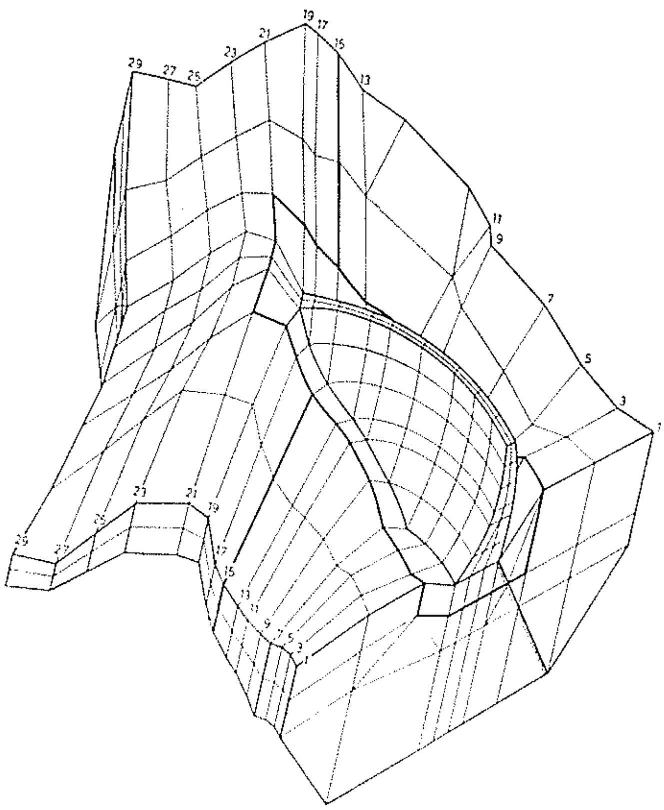

Fig. 14. Finite-element mesh

Owing to these settlements, the model showed a marked static contribution of the arches indicating that the dam finds a compensating support in the two rock abutments.

The fault showed a tendency to close under the action of hydrostatic load. During failure tests, involving an increase in the hydrostatic load, collapse was finally reached by sliding on the laminated layer under the bottom of the dam at a value of 3.5 times the normal water loading conditions.

4.2 Stability Analysis by Limit Equilibrium Method

To ascertain the existence of satisfactory safety conditions of the foundation rock mass, a stability analysis was deemed advisible taking into account the final conditions of the rock mass after excavation works. Limit

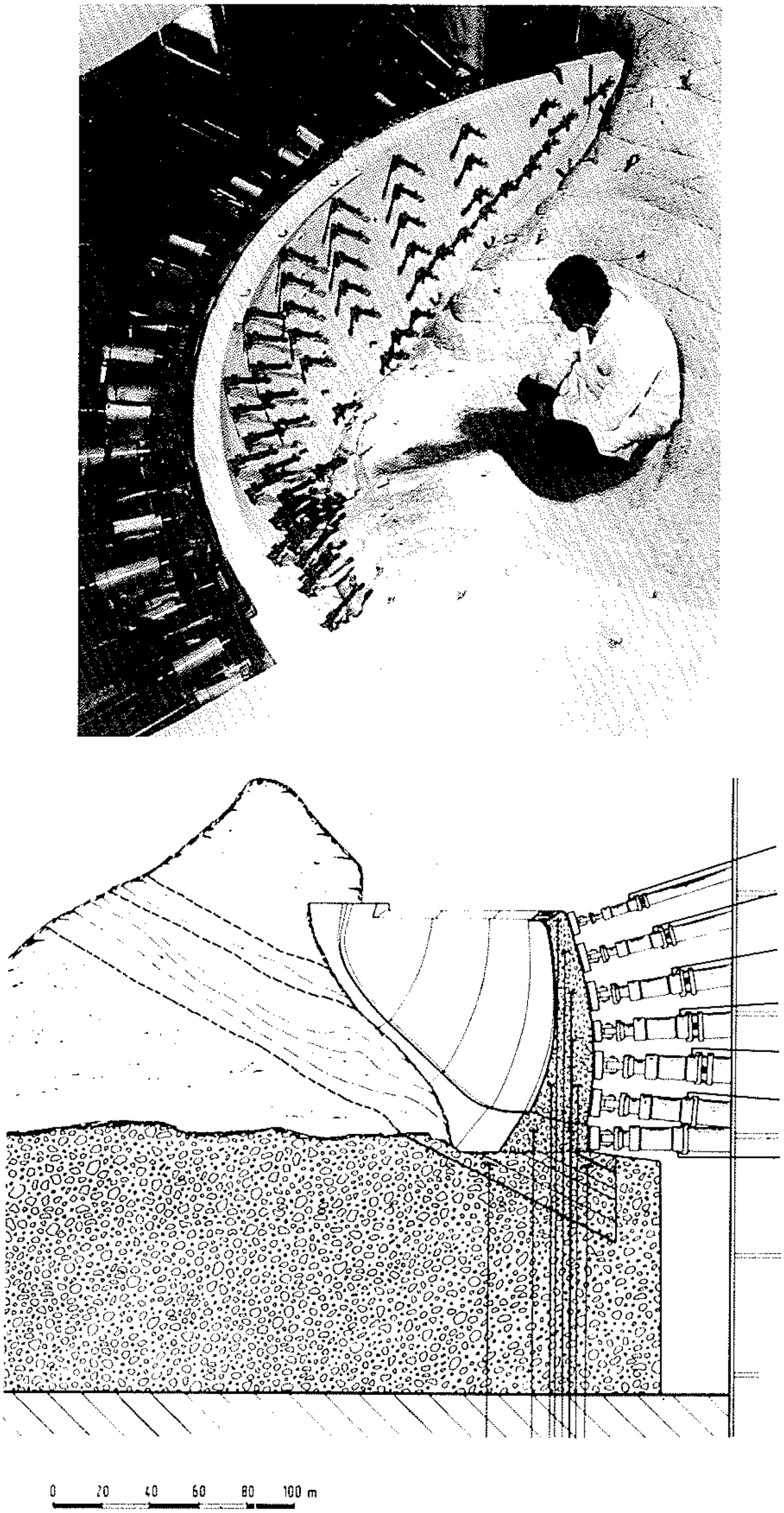

Fig. 15. View of the geomechanical model and the loading arrangement simulating dead weight and water thrust

equilibrium analysis was used assuming that possible sliding might occur at the abutments, along weak surfaces of the rock mass, which, in this case are identified with the bedding planes (*ST*) and the joint system (*KI*) (Fig. 16).

In addition to the self weight (*W*) of the minimum reacting wedge related to bedding planes (*ST*) and joint system (*KI*), external forces like water pressure on joints (*Ust*) and (*Uki*) and the resultant thrust (*S*) applied by the dam has been considered for the stability analysis.

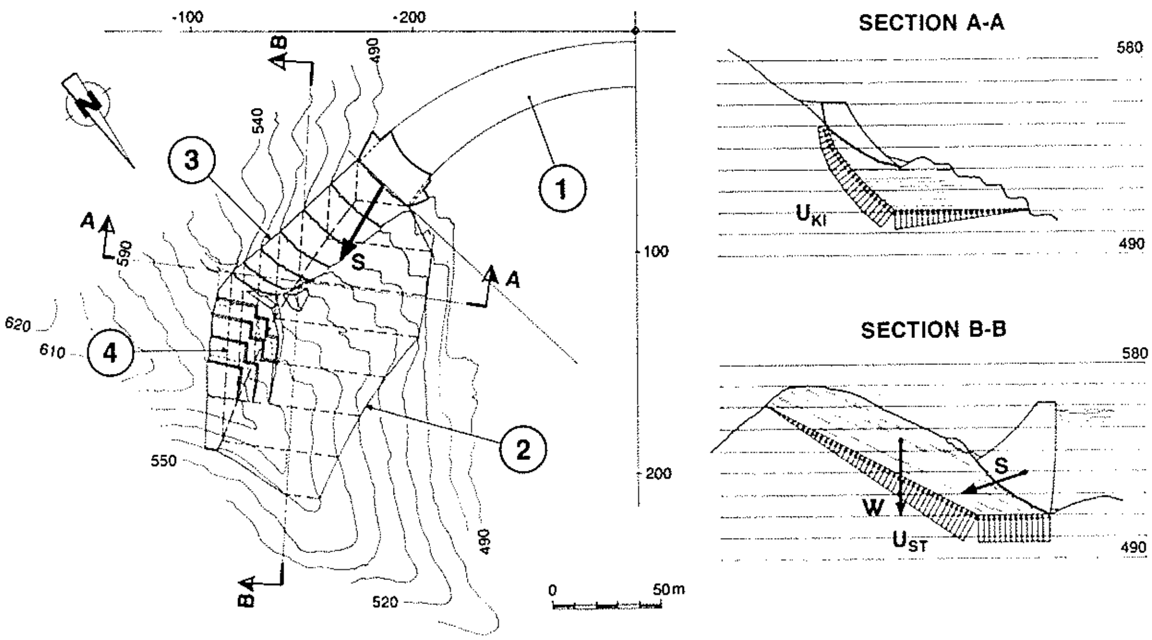

1	- ARCH OF THE DAM
2	- POTENTIAL SLIDING PLANE DEFINED BY LAYERS **(ST)**
3	- POTENTIAL SLIDING SURFACE DEFINED BY JOINT SET **(KI)**
4	- CONSOLIDATION WORKS (CONCRETE BERMS)
$\vec{S}$	- ARCH DAM THRUST
$\vec{U}_{ST}, \vec{U}_{KI}$	- WATER PRESSURE ON JOINTS **ST** and **KI**
$\vec{W}$	- SELF WEIGHT OF THE WEDGE

Fig. 16. Models for the limit equilibrium analysis of the right abutment

Since the location of a possible sliding is not known a priori, stability checks were carried out for several possible mechanisms, assuming the hypothesis of sliding starting at elevations increasing by 10 m from toe to crest. The most probably sliding mechanism will, of course, be that for which the safety factor (*FS*), defined as ratio of resisting forces to the driving ones, assumes a minimum value.

The following design parameters have been assumed:

— Bedding planes (*ST*): $\varnothing\ st = 13^0$ degrees, $Cst = 0$ MPa
— Joint system (*KI*): $\varnothing\ ki = 35^0$ degrees, $Cki = 0$ MPa

It was assumed that the drainage system and the grout curtain involved a decrease of 50% of max uplift effect that could occur on sliding planes.

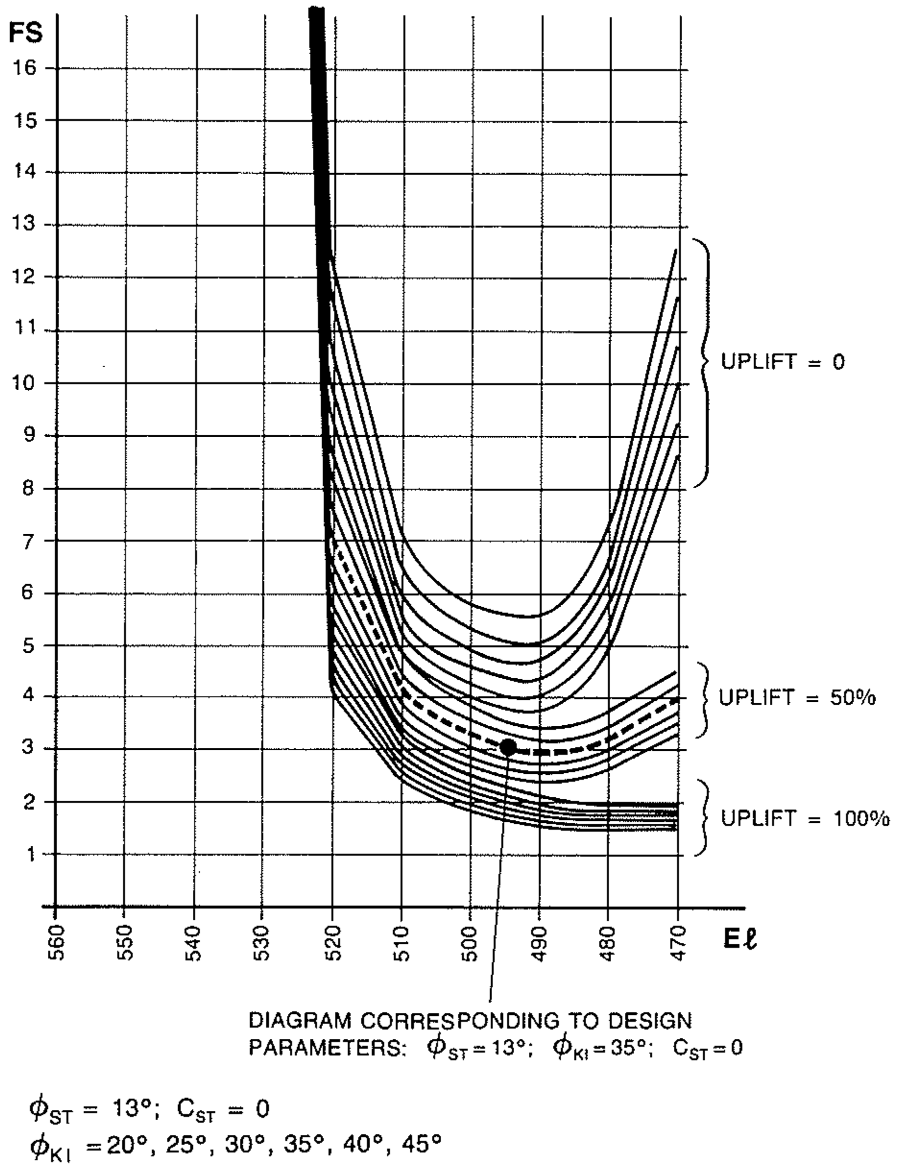

Fig. 17. Limit equilibrium analysis of the right abutment. Safety factor versus elevation of the potential sliding surface

It seemed advisible to analyse the stability conditions of the abutment rock mass assuming conservative values of strength parameters. For this reason it was assumed zero cohesion and a value of the friction angle on the bedding planes equal to 13⁰, corresponding to the minimum value determined on laminated layers.

The stability analysis was also performed taking into account a seismic event with a horizontal acceleration of 7% of gravity in horizontal direction and 10% in vertical direction.

The criterion has been adopted that the values of safety factor should be higher than 2 (static conditions) and 1.5 (seismic event); for this reason it was necessary to plan some stabilizing measures.

The solution of increasing the self weight (W) by means of concrete was adopted. Some concrete berms were cast above el. 540 m at the right abutment (weight about 140 MN) and at the left abutment in the area with the fault (weight about 330 MN). Some prestressed rock anchors for a total force of 53 MN were installed to bind the two edges of the fault which had previously been consolidated by replacing the filling material with concrete down to a depth of 20 m.

The results of the parametric studies including the effect of the stabilizing works is shown in Fig. 17 which refers to the right abutment. The safety factor is shown as a function of elevation of the potential sliding surface. The different diagrams are relevant to uplift variations and possible changes of friction angles on *KI* joints. It must be observed that the results shown in the figure are referred to the limit case of dam behaviour as "Independent Arches" which can be assumed as the ultimate behaviour of the dam before collapse.

Fig. 18. View of the foundation rock at the right abutment

5. Excavation Stability

Dam foundation excavation, especially at the right abutment, was one of the main problems to be solved during the construction of the dam. Owing to the structural features of the formation (layers dipping downhill, toward the excavation: see Fig. 18) unstable equilibrium conditions of the downstream wall were determined, with possibility of slide of substantial rock volumes.

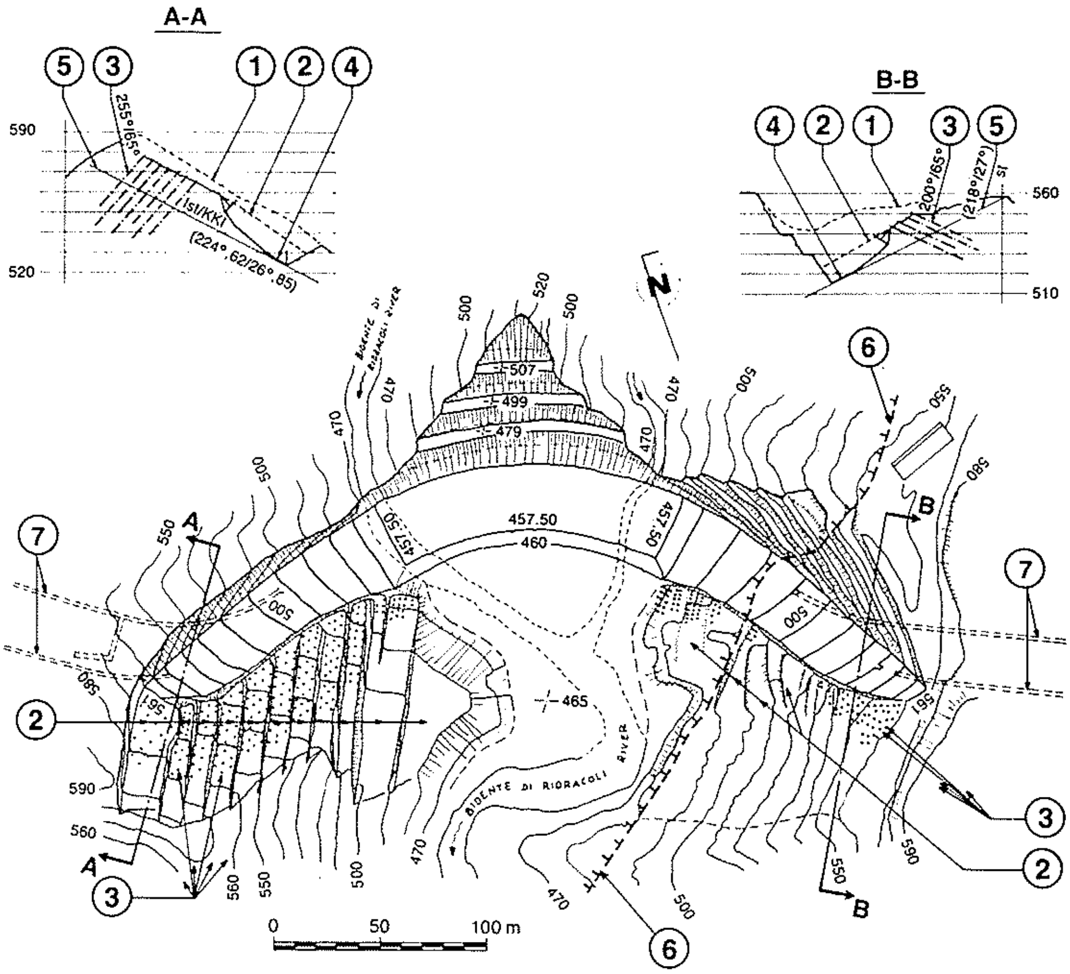

1 - ORIGINAL GROUND PROFILE
2 - 1st STAGE EXCAVATION
3 - PRESTRESSED ROCK ANCHORS
4 - 2nd STAGE EXCAVATION
5 - POTENTIAL SLIDING SURFACE
6 - FAULT OUTCROPPING LINE
7 - ROCK TREATMENT GALLERY

Fig. 19. Stages of rock excavation and reinforcing measures

Main dimensions of the right abutment excavations may be summarized as follows:

- wall length: about 100 m;
- average wall height: about 20 m;
- horizontal thickness variable between 10 m at the top and 38 m at the toe.

The upstream wall did not present any particular stability problems as the rock formation dipped uphill in relation to the excavation.

During the first month of work at the site, four excavation methods were studied (Bavestrello, 1983) and appraised both in terms of cost and working period. The most advantageous solution (see Fig. 19) involved a full face excavation method according to the following phases:

1 a) deep stripping of topsoil and formation of berms following the rock structure (bedding planes *ST* and fracture joint *KI*);

1 b) placing of prestressed anchors, located outside the dam foundation area, on the downstream rock surface shaped as berms;

2 a) full face final profile excavation in stabilized rock, starting from the dam crest elevation towards the river bed.

The volume of rock mass at the right abutment affected by the excavation (stability) was approx. 111 000 m^3.

The statical calculation of the equilibrium conditions of the rock mass has been developed both biaxially (sliding only along bedding planes *ST*), and triaxially i. e. taking into account possible slide parallel to the intersection line of the joint systems *ST* and *KI* (wedge failure). Fig. 20 shows the results of three dimensional graphic analysis with the indication of the limit equilibrium curve ($FS=1$) which defines the "stability zone" ensured only by the friction effect (the contribution of the cohesion was not taken into account). It can be observed that the point (W), which represents the resultant of the forces in a natural condition, lies outside the stability zone. Therefore a stabilizing force must be introduced.

A safety factor (FS) equal to 1.2 was assumed taking into account the temporary stabilization required.

The stabilizing force (A) and its orientation were determined by numerical methods improved by optimization criteria in order to define the best combination between the "Anchor Efficiency Factor" (EA) and the "Anchor Length Factor" (LA); where (EA) represents the sliding resistance exerted by the unit anchor force and LA represents the active length of the anchors needed for the unit thickness of the rock wedge to be stabilized.

The values of the total stabilizing force were calculated:

$$|A| = 960\,000 \text{ kN}$$
$$\text{orientation: } (255^0, 25^0).$$

This force was applied by means of a great number of prestressed anchors having an average length of 37 m.

— 1800 kN bearing capacity: 503 pieces;
— 1500 kN bearing capacity: 40 pieces.

The distribution of these forces along the wall of the excavation is shown in Fig. 19. The heads of the cables are shown in Fig. 21. The anchors were arranged to allow prestressing at any time, during the whole construction (at least 5 years). Each cable (see Fig. 22), being covered along the active section by anti-corrosion and lubricating materials, could slide inside a protective 2 mm-thick polyethylene wrapping. The anchor fixing was achieved by grouting the steel cables for a length of 12 m (1800 kN) and of 8 m (1500 kN). To avoid stress concentration in the rock mass at the same depth from the surface, the length of the cables was alternately changed.

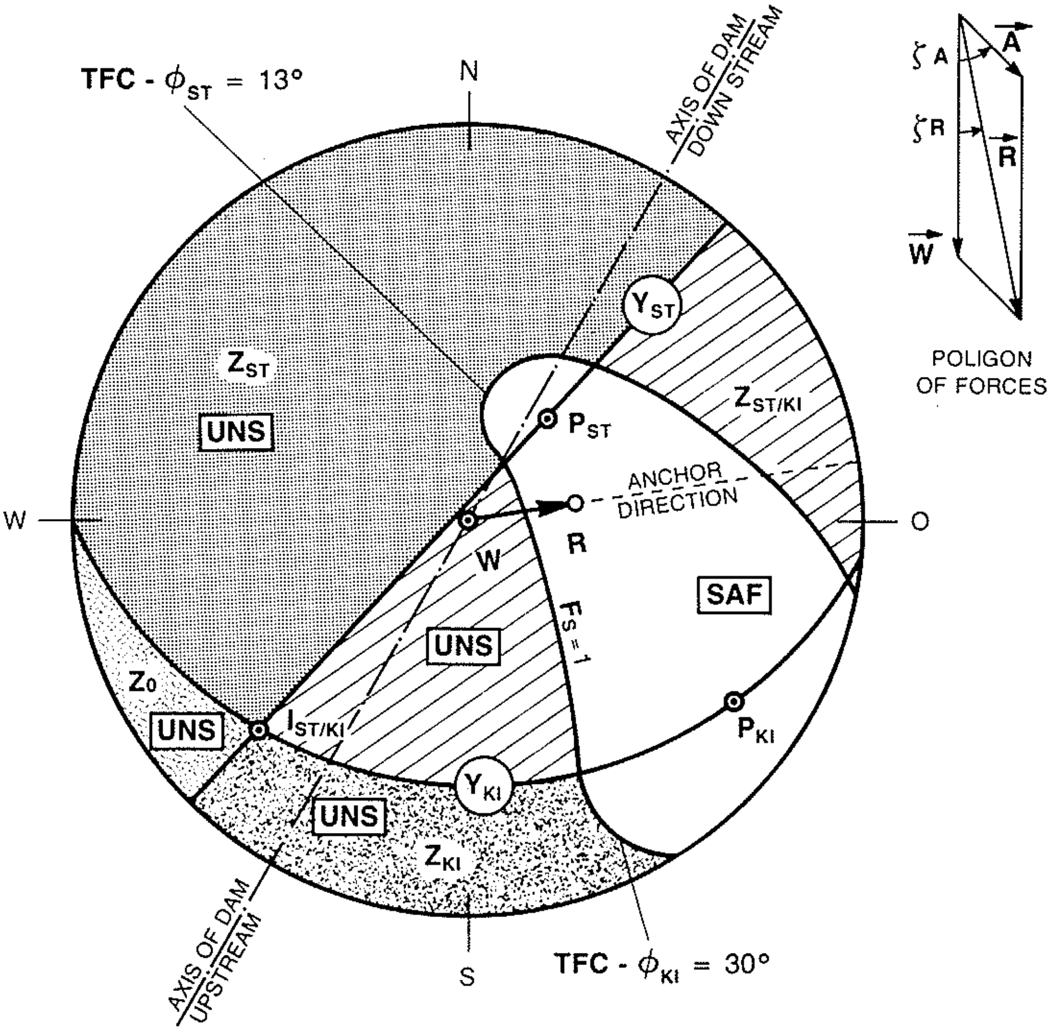

P_{ST}, P_{KI}	- POLES
TFC	- TALOBRE'S FRICTION CONES
SAF	- SAFE
UNS	- UNSAFE
$\vec{W}$	- WEIGHT
$\vec{A}$	- SUPPORTING FORCE INTRODUCED BY POST-TENSIONED ROCK TENDONS
$\vec{R}$	- RESULTANT
Z_{ST}	- BLOCK SLIDING ALONG JOINT **ST**
Z_{KI}	- BLOCK SLIDING ALONG JOINT **KI**
$Z_{ST/KI}$	- WEDGE SLIDING ALONG **ST** AND **KI**
Zo	- UNSEATING OF BOTH PLANES

Fig. 20. Graphical stability analysis of right abutment excavations (lower hemisphere)

The tendon's head is formed by a steel bearing plate and by a thick steel collar tube grouted into the rock.

Excavations were made by smooth blasting in order to obtain well shaped surfaces and to minimize disturbance to the bedrock. Fully grouted bolts (length 3—8 m) were mainly used to stabilize surface layers. In order to minimize weathering, especially of the marl, an 11 000 m^2 shotcrete protection having an average thickness of 100 mm reinforced with wire net, was provided on the berms.

Fig. 21. View of the right abutment. The arrangement of the prestressed anchors on the berms is shown

The volume of rock excavated at the right abutment amounted to 116 000 m^3, in the first stripping phase and to 65 000 m^3, in the second phase (deep excavation). For the whole dam foundation 500 000 m^3 of the rock were excavated.

Upon completion of the dam construction anchor loads were partially reduced at the upper four berms at the right abutment, in order to avoid the dam thrusting onto the rock wedge of Fig. 16, causing a decrease in the safety factor.

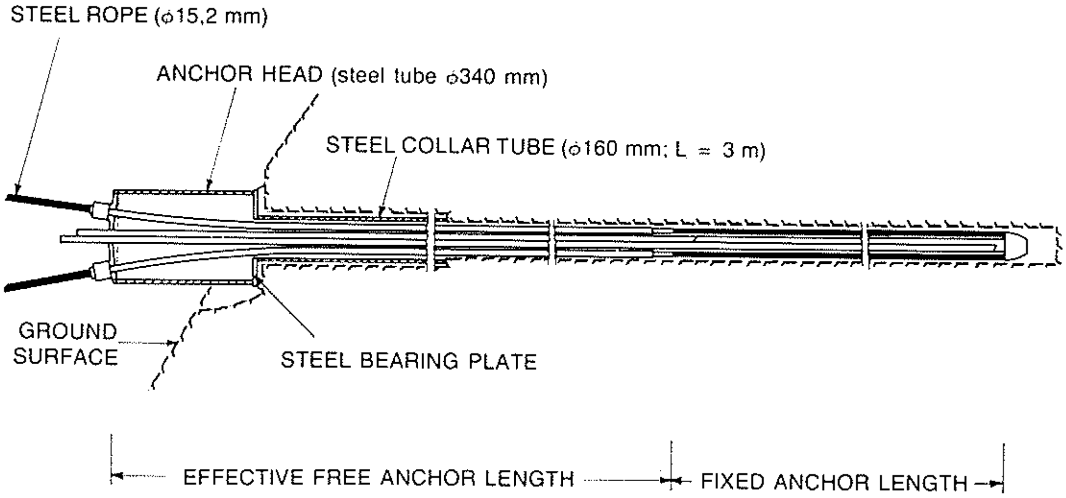

Fig 22. Corrosion resistent tendon

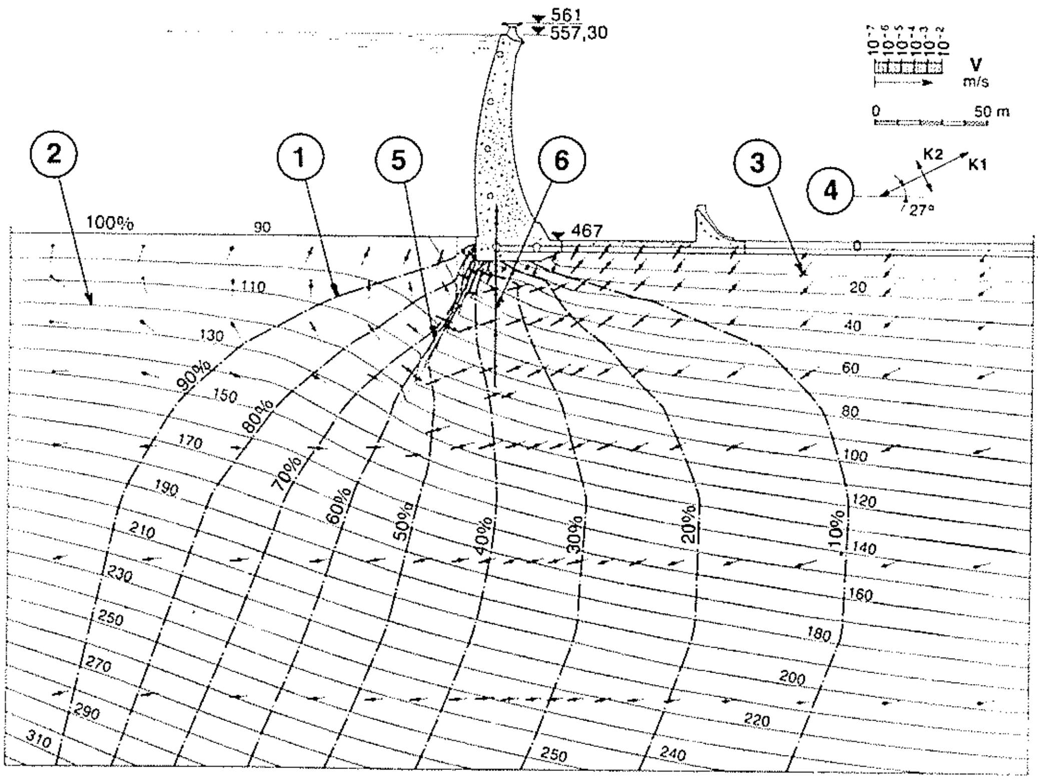

Fig. 23. Hydraulic flow-net: main section of the dam

6. Seepage Problems of the Rock Foundation

The marl-sandstone formation exhibits a relatively low permeability. Given the low sliding strength of some laminated layers and the marked influence of possible uplift effect on the stability of the whole dam, it was felt advisible to study the hydraulic flow net due to reservoir filling. The study was performed by 2D-FEM models assuming a hydraulic anisotropy characterized by the following values of the conductivity coefficient ($K1$) and ($K2$).

$K1 = 2.7 \times 10^{-6}$ m/s parallel to bedding planes,
$K2 = 0.9 \times 10^{-6}$ m/s normal to bedding planes.

The values of the parameters were evaluated on the basis of "in situ" test results with the aid of an electrical analogy. The study was carried out for two of the most representative vertical sections, one of which (Fig. 23)

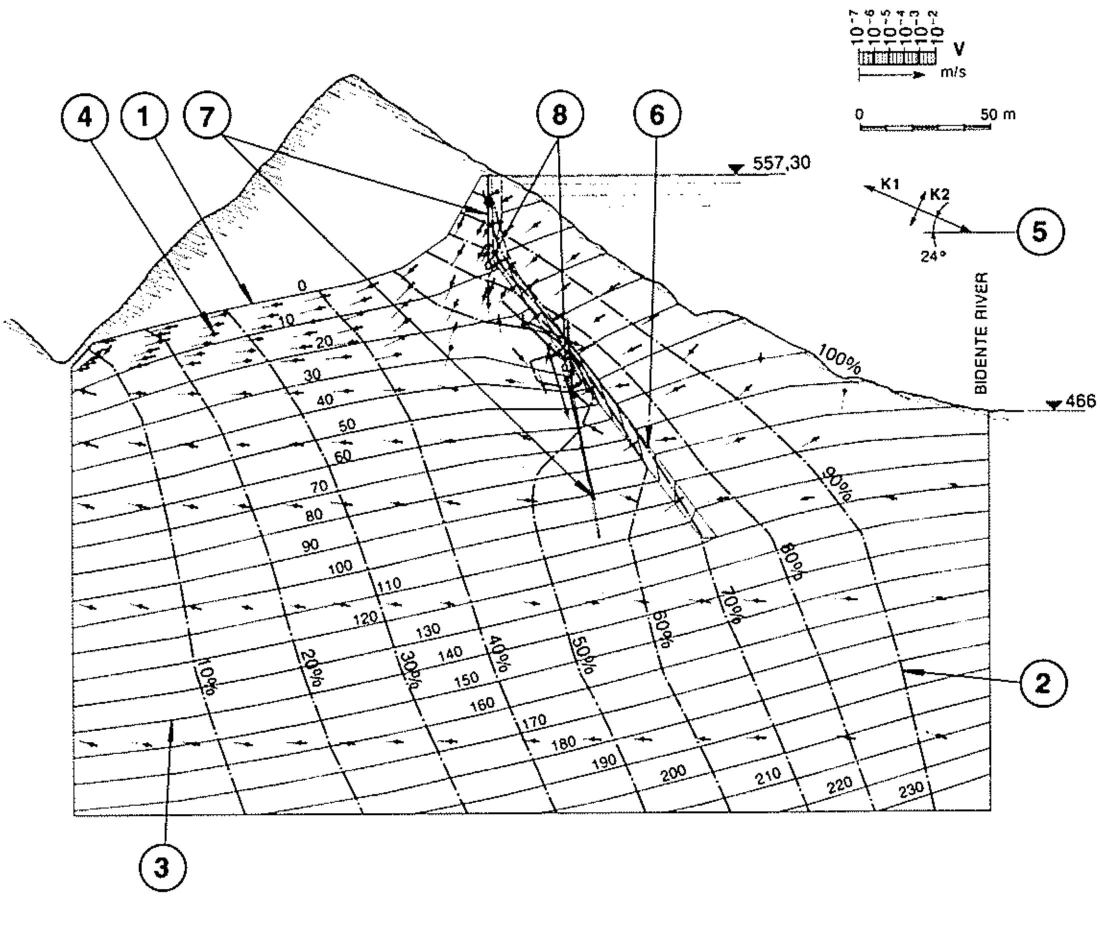

1 - WATER TABLE
2 - EQUIPOTENTIAL LINE
3 - EQUAL PRESSURE LINE
4 - FLOW VELOCITY
5 - DIRECTION OF HYDRAULIC CONDUCTIVITIES
6 - GROUT CURTAIN
7 - DRAINAGE NET WORK
8 - ROCK TREATMENT GALLERY

Fig. 24. Hydraulic flow-net: right abutment cross section

concerns the main section of the dam (flow problems only), and the other (Fig. 24) concerns the right abutment rock body (flow and free surface problems). The improvement achieved by rock consolidation and curtain grouting has been taken into account, simulating the treated rock as an isotropic permeable medium with coefficient $K = 1.5 \times 10^{-7}$ m/s (about 1 Lugeon unit). The analysis of the results, shown in Fig. 23 and 24, has indicated that:

— the anisotropy value, i. e. the ratio $K1/K2$ and the flow direction, act favourably by reducing uplift pressures (with respect to the isotropic hypothesis) moving equipotential lines upstream;
— the waterproofing grout curtain (inclined 30° upstream and with a depth of 75 m) and consolidation works around the pulvinus with a thickness of 10 m involve a slight uplift reduction, due to the low natural permeability of the rock mass;
— the introduction of a drainage network in combination with grout curtain involves a further uplift reduction which induces an additional shift of equipotential lines upstream.

The influence of the grout curtain may be noted by the sudden drop of equal pressure lines. The extent of this drop is on average around 15 m, with a max. of 25—30 m.

As regards the flow through the right abutment, Fig. 24 shows that the water table level inside the rock body presents an initial marked drop, then it goes on towards the adjacent small valley with 20% slope; the flow rates at the side of the valley is negligible. The same figure shows the remarkable flows conveyed by galleries and drainages, especially at the lower gallery.

Foundation treatment works (Fig. 25) were designed and carried out as follows (Bavestrello et al., 1985):

— *Consolidation Grouting*

Along the whole foundation surface for an average depth of 10 m, grout holes (46 mm diam) were drilled from the pulvinus and from the perimetral gallery. The grout holes were divergent in order to obtain an average spacing 5×5 m at the contact between the pulvinus and the foundation rock mass. Grouting started after the pulvinus had been completed with the aim of treating the contact between the basal concrete and the foundation rock surface. Grouting was carried out with ascending method in-stags varying from 3 to 5 m with the same pressure of 1 MPa.

The overall length was about 41 000 m and the lineal grout take was on average 300 N/m.

— *Grout Curtain*

The 75 m-deep grout curtain in the central zone, was also extended inside the two abutments for some 200 m through adits at intermediate

elevations, and inclined in the upstream direction in order to take advantage of the stabilizing component due to hydrostatic thrust.
Grout curtain holes (46 mm diam) were arranged in two divergent rows (Fig. 25) and spaced 4 m on each row. The inclinations of upstream and downstream rows with respect to the vertical were respec-

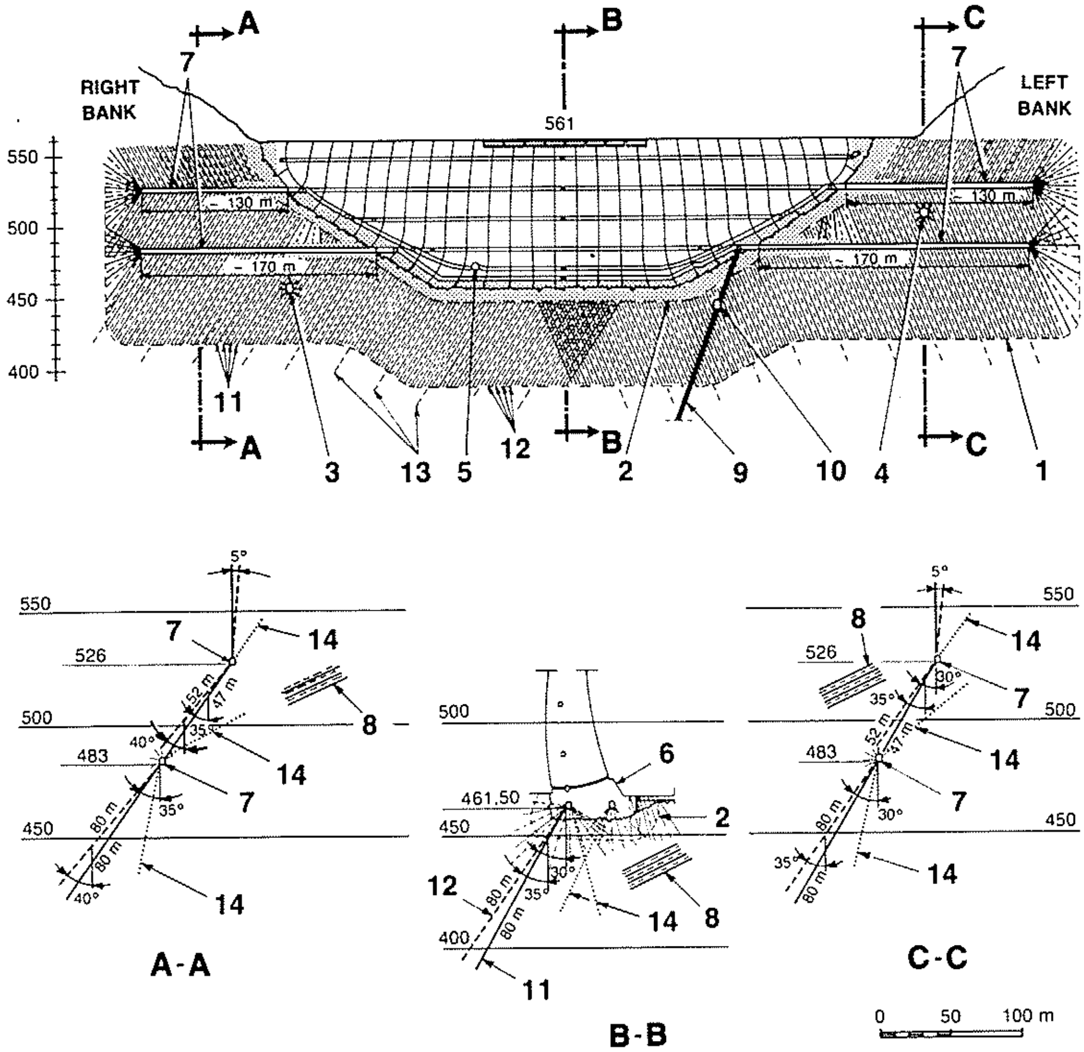

1 - INDICATIVE CONTOUR OF WATERTIGHT SCREEN
2 - CONSOLIDATION INDICATIVE CONTOUR
3 - LOW-LEVEL OUTLET
4 - MID-LEVEL OUTLET
5 - RESERVOIR DRAIN
6 - PULVINUS
7 - ROCK TREATMENT GALLERY
8 - BEDDING PLANES (ST)
9 - FAULT PLANE
10 - FAULT IMPROVEMENT GALLERY
11 - 1st SERIES HOLES (1 EVERY 4 m)
12 - 2nd SERIES HOLES (1 EVERY 4 m STAGGERED BY 2 m IN RELATION TO 1st SERIES HOLES)
13 - PILOT HOLES (1 EVERY 20 m)
14 - DRAINAGE HOLES (1 EVERY 6 m)

Fig. 25. Grout curtain, stabilization and drainage

tively 35^0 and 30^0. The holes were directed in order to involve as many rock joints *KI* as possible, which represents the most potential seepage path.

Grouting was carried out with ascending method in stags 5 m long. The grout mix was composed of cement, bentonite (2%) and a water cement ratio generally of 2 : 1 changing to 1 : 1 when the absorption was greater than 1 kN/m. The grouting pressure was adjusted to depth from a minimum value of 1 MPa to a max of 3 MPa.

The max values of grouting pressure at each depth were verified on the base of "in situ" fracturing tests.

During the whole grouting phase the deformations of the rock mass were controlled by means of borehole extensometers.

The total surface of the grout curtain was about 60 000 m^2, with an overall length of drilling of about 48 000 m. The average lineal grout take was about 360 N/m. The efficiency of the grout curtain was verified by means of in situ permeability tests which showed a reduction of permeability of 80% to 100%. A permeability value lower than 1 Lugeon was obtained in all the treated rock mass.

— *Drainage*

To prevent possible uplift effects a dense drainage hole system was built downstream of the grout curtain and at the downstream toe of the dam. Fig. 25 shows the arrangement of the drainage holes in the central zone and in the two abutments. A total of 158 holes (110 and 85 mm diam, spaced 6 m) were drilled with a total length of 6 800 m. The drains were equipped with microfessured PVC pipes and the space between the borehole wall and the pipe was filled with fine sand in order to increase the life of the drains.

References

Bavestrello, F. (1983): Stabilizzazione temporana degli scavi d'imposta della diga di Ridracoli — A. G. I., XV National Meeting of Geotechnique, Spoleto, Italy.

Bavestrello, F., Marini, P. P. (1985): Construction of the Ridracoli Dam. Water Power & Dam Construction, July, 1985.

Fumagalli, E. (1977): Geomechanical Models for Rock Abutments — A. G. I., International Symposium "The Geotechnics of Structurally Complex Formations", Capri, Italy.

Oberti, G., Carabelli, E., Goffi, L., Rossi, P. P. (1979): Study of an orthotropic rock mass: experimental techniques, comparative analysis of results, ISRM IV International Congress, Montreux, Switzerland.

Oberti, G., Goffi, L., Rossi, P. P. (1983): Study of Stratified Rock Masses by Means of Large-scale Tests with a Hydraulic Pressure Chamber, ISMR V International Congress, Melbourne, Australia.

Rebaudi, A. (1978): Cenni informativi circa le indagini e le prove esperite per la ricerca delle proprieta fisiche e meccaniche della roccia di fondazione della diga di Ridracoli — A. G. I., XIII National Meeting of Geotechnique, Merano, Italy.

Rossi, P. P. (1980): Analisi del comportamento deformativo di ammassi rocciosi stratificati mediante prove con camera idraulica — A. G. I., XIV Meeting of Geotechnique, Firenze, Italy.

Vogt, F. (1925): Über die Berechnung der Fundamentformation — Norske Videnskaps Akademi, Oslo, Norway.